

# Homogeneity and Size Effects on the Liquid-Gas Coexistence Curve

Al. H. Raduta<sup>1,2</sup>, Ad. R. Raduta<sup>1,2</sup>

<sup>1</sup>*GSI, D-64220 Darmstadt, Germany*

<sup>2</sup>*NIPNE, RO-76900 Bucharest, Romania*

The effects of (in)homogeneity and size on the phase diagram of Lennard-Jones fluids are investigated. It is shown that standard multifragmentation scenarios (finite equilibrated systems with conserved center of mass position and momentum) are implying a strong radial inhomogeneity of the system strongly affecting the phase diagram. The homogeneity constraint is therefore necessary for finite systems in order to align to the “meaning” of infinite systems phase diagrams. In this respect, a method which deduces the equation of state of homogeneous finite systems from the one corresponding to bulk matter is designed. The resultant phase diagrams show a strong dependence on the system’s size.

PACS numbers: 24.10.Pa; 25.70.Pq; 21.65.+f

Phase transitions have been studied from a long time in the limit of infinite matter. However, there are many physical situations away from the thermodynamic limit at both microscopic and macroscopic scales. Such systems are presently of special interest as so far there is little knowledge about their thermodynamical behavior. There are thus fundamental questions related to these systems such as whether they do present phase transitions and, if yes, how can these be identified. (Recent attempts to extend the standard thermodynamics towards the “small” systems can be found in Refs. [1, 2, 3, 4].)

Highly excited nuclear systems are good “laboratories” for thermodynamics studies. Due to the van der Waals type of the nucleon-nucleon interaction these systems are supposed [5] to exhibit a liquid-gas phase transition as the classical fluids. The connection is however not straight forward due to their (relatively) small number of constituents and the presence of the (long-range) Coulomb force. The effect of the Coulomb interaction on the nuclear liquid-gas phase transitions was studied previously (see e.g. Refs. [4, 6]). The effects of other features specific to multifragmentation such as finite size (for attempts to address the finiteness of the system within Hartree-Fock theories see e.g. Refs. [7, 8]) and degree of homogeneity are still mostly unknown. These aspects are addressed in the present paper.

The classical Lennard-Jones 6-12 (LJ) fluid is used for illustrating the paper’s ideas. While neglecting for the quantum effects acting in nuclear matter, it has the advantages of generality and tractability. The LJ potential writes:

$$v_0(r) = 4\epsilon \left[ \left( \frac{\sigma}{r} \right)^{12} - \left( \frac{\sigma}{r} \right)^6 \right] \quad (1)$$

Two versions of the above potential are considered herein. The first is the truncated and shifted (TS) LJ potential:  $v(r) = v_0(r) - v_0(r_c)$  when  $r < r_c$ ;  $v(r) = 0$  when  $r \geq r_c$ . The second is the truncated and long range corrected (TLRC) LJ potential:  $v(r) = v_0(r)$  when  $r < r_c$ ;  $v(r) = 0$  when  $r \geq r_c$ , corrections being subsequently included in

order to account for the effect of the neglected tail [12]. In the present work we use  $r_c = 2.5 \sigma$ . Phase diagrams of such fluids are subsequently constructed for various situations. Phase transitions in finite systems being here addressed, an adequate representation is necessary in order to identify them. For example, the  $P(V)|_T$  curves corresponding to an isochore canonical ensemble will prompt the (first order) phase transition through backbendings *even in the case of small systems* [4, 9]. Pressure can be easily evaluated starting from its canonical definition:  $P = T \partial \ln Z(\beta, V) / \partial V$ , where  $Z(\beta, V)$  is the system’s canonical partition function:

$$Z(\beta, V) = \frac{1}{A! \lambda_T^{3A}} \prod_{i=1}^A \int d\mathbf{r}_i \exp \left( -\beta \sum_{i<j}^A v(r_{ij}) \right), \quad (2)$$

where  $\beta \equiv 1/T$  and  $\lambda_T$  is the thermal wavelength. The result is the following virial expression:

$$P = \frac{AT}{V} - \frac{1}{3V} \left\langle \sum_{i<j}^A r_{ij} \frac{\partial v(r_{ij})}{\partial r_{ij}} \right\rangle, \quad (3)$$

where  $\langle \rangle$  has the meaning of canonical average. When conservation of the system’s center of mass (c.m.) and c.m. momentum is also considered in  $Z(\beta, V)$ , one simply has to change  $A$  into  $A - 1$  in eqs. (2) [the power of  $\lambda_T$ ] and (3) [the first term]. While rather redundant for very large systems ( $A \rightarrow \infty$ ), these constraints give important effects when dealing with small systems. Expressions like (3) can be easily evaluated by means of Metropolis simulations. Knowing the formal expression of  $Z(\beta, V)$ , (2), the statistical simulation of the corresponding canonical ensemble at constant volume is straight-forward: Pick a randomly chosen particle and make a random variation of its initial position (in a fixed interval  $\Delta V$ ). Then, consider this move according to the acceptance  $\exp(-\beta \Delta v_t)$ , where  $\Delta v_t$  is the change in the system’s total potential energy. The simulation can be easily adapted to the case of the conserved system’s c.m. and c.m. momentum: Two randomly chosen particles are moved simultaneously

with  $\Delta \mathbf{r}$  and  $-\Delta \mathbf{r}$  such that the system's c.m. remains fixed ( $\Delta \mathbf{r}$  being a variation randomly chosen in the volume interval  $\Delta V$ ). Then, the move is considered according to the same acceptance.

The present study is started by considering the case of a system at fixed temperature  $T$ , composed of  $A$  particles interacting via TS LJ potential, contained into a spherical recipient of volume  $V$ , having the c.m. constrained to coincide with the center of the recipient. The corresponding canonical ensemble is simulated as described earlier. Then, isothermal  $P(V)$  curves can be evaluated by means of eq. (3), adapted to the considered conservation laws. Subsequently, the borders of the liquid-gas coexistence region are evaluated by performing Maxwell constructions on all  $P(V)|_T$  curves bending backwards. The resulting phase diagrams (in temperature vs. density representation) corresponding to two systems of different sizes  $A = 20$  and  $A = 50$  are represented in the upper part of Fig. 1. The increase of the critical temperature with the system's size can be observed. A striking feature of these phase diagrams is the small densities corresponding to the borders of the liquid-gas coexistence regions. In this respect, note that the liquid border is situated at densities smaller than  $0.2 \sigma^{-3}$  which differs a lot from the LJ phase diagrams corresponding to infinite homogeneous systems [10] where the liquid border goes up  $0.8 \sigma^{-3}$ . The reason for this discrepancy can be easily understood from the lower part of Fig. 1. There, the radial density profiles corresponding to three sample points chosen from the coexistence line of the  $A=50$  system are represented. In all three cases the system appears to be inhomogeneous, its density varying from higher values (towards the center of the recipient) to very small ones (towards the recipient's walls). The low density tails of these radial profiles are therefore inducing the above mentioned effect on the global density of the system (calculated as  $A/V$ ). In particular, note that at small values of the distance from the recipient's center the densities of the considered sample points tend to be consistent with the ones from Ref. [10]. Obviously, this inhomogeneity effect is dictated by the c.m. conservation constraint which forces the larger clusters to stay towards the center of the recipient and the smaller ones towards the borders. This example is particularly important in the context of multifragmentation where the system's c.m. is naturally conserved from event to event and similar density profiles are expected to occur.

Therefore, in order to meaningfully compare the phase diagram calculated for finite systems with the ones corresponding to infinite systems an extra constraint has to be imposed: *the homogeneity*. The infinite and homogeneous system can be simply approached within the (above-described) Metropolis simulation by implementing a cubic recipient with periodic boundary conditions (PBC). (No c.m. conservation constraint has to be imposed.) A number of 200 particles interacting via TLRC

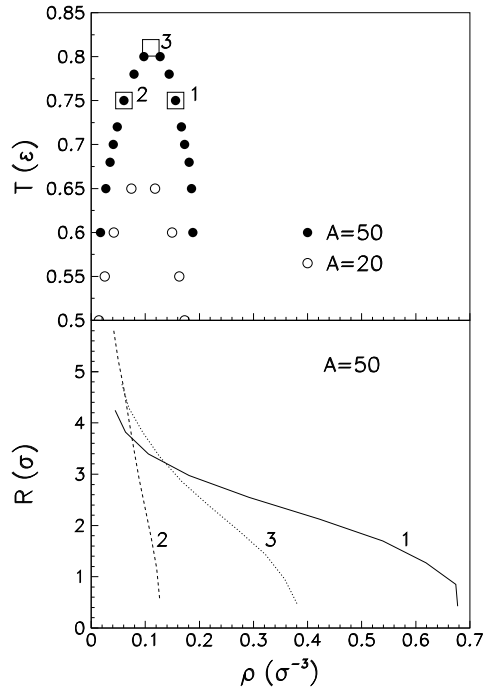


FIG. 1: Upper panel: Phase diagrams for two systems ( $A = 20$  and  $A = 50$ ) with conserved c.m. position and c.m. momentum. Three sample points from the  $A = 50$  phase diagram are represented by squares. Lower panel: Radial density profiles corresponding to the sample points from the upper part of the figure. The correspondence between curves and sample points is given by numbers.

or TS LJ potentials are placed in a cubic box with PBC. The very good agreement between our calculated phase diagram corresponding to the TLRC case (see Fig. 3, the “ $\infty$ ” curve) and the one from Ref. [10] is confirming the accuracy of the method here employed. The PBC simulations are used for evaluating the bulk “virial energy” per particle, defined as:

$$\mathcal{V} = \frac{1}{3A} \left\langle \sum_{i < j}^A r_{ij} \frac{\partial v(r_{ij})}{\partial r_{ij}} \right\rangle \quad (4)$$

Eq. (3) can be now translated into:

$$P = \rho (T - \mathcal{V}), \quad (5)$$

where  $\rho$  is the system's density. Therefore, in an infinite and homogeneous system, the virial energy per unity of volume can be written as:  $\tilde{\mathcal{V}} = \rho \mathcal{V}$ . Given the above definitions one may perform surface corrections for evaluating the  $\mathcal{V}$  term corresponding to finite systems. Since the system is supposed to be homogeneous, its total virial energy can be expressed as the difference between a bulk term and a surface one:

$$\mathcal{V}_t = \mathcal{V}_b (A - A_s f) = \tilde{\mathcal{V}}_b (V - V_s f), \quad (6)$$

where the index  $b$  specifies that the respective term is a bulk one,  $A_s$  and  $V_s$  are respectively the number of par-

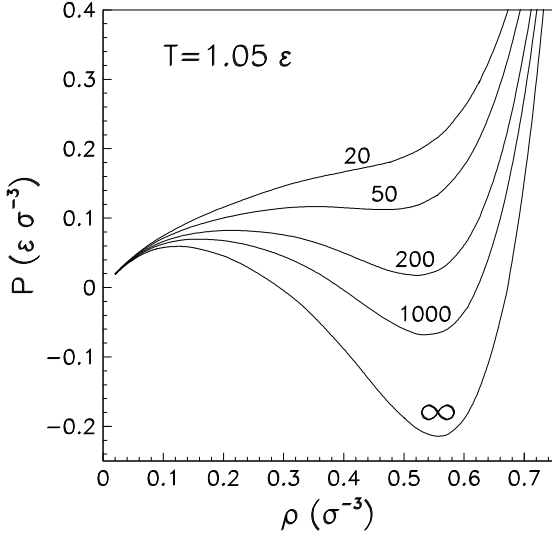


FIG. 2: Pressure versus density curves corresponding to systems of various sizes ( $A$ ) at fixed temperature,  $T = 1.05\epsilon$ , evaluated with eq. (5). The corresponding size of the system is specified on each curve.

ticles from the surface and the “volume” of the surface, and finally,  $1 - f$  is the ratio between the virial energy of a particle from the surface and the virial energy of a bulk particle. While for very large values of the recipient’s radius ( $R$ )  $1 - f$  is rigorously equal to  $1/2$  (i.e. the particles on the surface have half the number of nearest neighbors they have in bulk), for small values of  $R$  (the case of small systems) curvature corrections have to be applied to this factor. In the spirit of the previous definition,  $f$  can be fairly approached by the ratio between the surface of spherical cap situated *outside* the recipient, corresponding to a sphere of radius  $\sigma$  having the center on the surface of the recipient and  $4\pi\sigma^2$ . After some algebraic manipulation one gets:

$$f = \frac{1}{2} \left( 1 + \frac{\sigma}{2R} \right). \quad (7)$$

Note that when  $R \rightarrow \infty$  then  $f \rightarrow 1/2$ . Considering the surface “width” equal to  $\sigma$  (i.e. no two particles from that region, situated on the same radius, attract each other) one can re-express eq. (6) as:

$$\mathcal{V}_t = \mathcal{V}_b A \left( 1 - \frac{\mathcal{V}_s}{\mathcal{V}} f \right), \quad (8)$$

so that:

$$\mathcal{V} = \frac{\mathcal{V}_t}{A} = \mathcal{V}_b \left\{ 1 - \frac{1}{2} \left( 1 + \frac{\sigma}{2R} \right) \left[ 1 - \left( 1 - \frac{\sigma}{R} \right)^3 \right] \right\}. \quad (9)$$

Eq. (9) can be further expressed in terms of  $\rho$  using the identity  $\sigma/R = [4\pi\rho\sigma^3/(3A)]^{1/3}$ . Subsequently, eq. (5) [with  $\mathcal{V}$  given by eq. (9)] can be applied for calculating the pressure of a finite system of size  $A$  at various values of  $\rho$ .

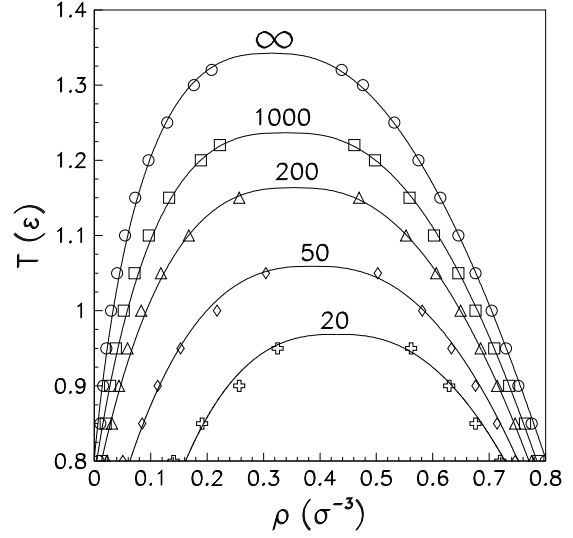


FIG. 3: Phase diagrams corresponding to the TLRC LJ fluid, corresponding to different sizes of the system. The system’s size is specified on top of each diagram. Points calculated via Maxwell constructions are represented with symbols. Full lines are fits of eq. (10) on the calculated points.

An illustration of the results of the method is given in Fig. 2 where  $P(\rho)|_T$  curves, corresponding to the temperature  $T = 1.05\epsilon$  are represented for various sizes of the system. One can observe that the depth of the backbending of the curve is diminishing as the size of the source is decreasing such that at system sizes as small as  $A = 20$  the backbending completely disappears.

Maxwell constructions have been further performed on the  $P(V)|_T$  curves corresponding to various values of  $T$  and  $A$  allowing thus the construction of phase diagrams for various sizes of the system. The results corresponding to the TLRC and TS LJ forms of potential are given in Figs. 3 and 4 respectively. The points from the coexistence region borders obtained via Maxwell constructions can be further interpolated in order to get an estimation of the critical point and a clearer view on the systems’ phase diagrams by means of the Guggenheim scaling relations for the coexistence curve:

$$\rho_{\pm} = \rho_c (1 + a \epsilon \pm b \epsilon^{\beta}), \quad (10)$$

where  $\rho_+$  corresponds to the liquid branch,  $\rho_-$  to the vapor branch of the coexistence curve,  $\rho_c$  is the critical density,  $\epsilon \equiv (T_c - T)/T_c$  ( $T_c$  being the critical temperature) and  $\beta$  is the critical exponent of the coexistence curve. Eq. (10) is fitted on the points obtained via the Maxwell construction method by adjusting the parameters:  $T_c$ ,  $\rho_c$ ,  $\beta$ ,  $a$  and  $b$ . As observed in Figs. 3 and 4 the quality of the obtained fits is very good. (It is worth mentioning that for the TS potential, infinite system case,  $\beta = 0.34$  which sharply corresponds to the liquid-gas universality class.) For both considered potentials the critical temperature is drastically decreasing and the critical density

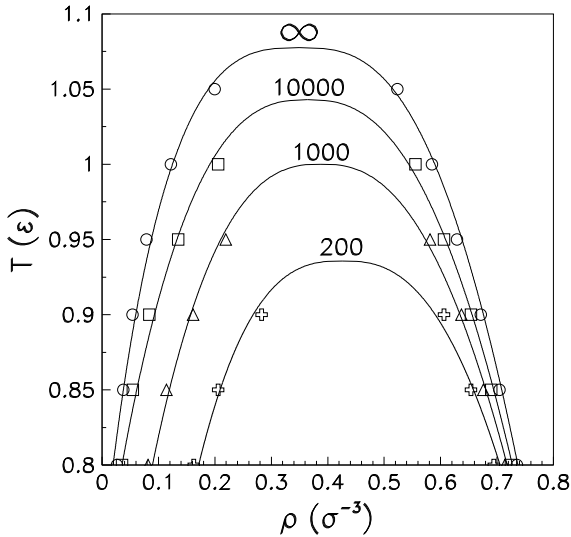


FIG. 4: Same as Fig. 3 but for a TS LJ fluid.

is increasing with decreasing the size of the source. In particular, note that important deviations from the “ $\infty$ ” phase diagram can be observed even for the phase diagram of a system as large as  $A = 10^4$  (see Fig. 4). This result is particularly important since it proves that thermodynamically the bulk limit is not (even by far) attainable in nuclear multifragmentation experiments (where the equilibrated systems formed are usually smaller than  $A = 300$ ).

Summarizing, homogeneity and size effects on the system’s phase diagram have been discussed in the framework of the classical LJ fluid. Phase diagrams are constructed using a method adequate for revealing the coexistence region even for small systems: Maxwell constructions on canonical  $P(V)|_T$  curves. It was shown that standard scenarios like finite systems with conserved c.m., physically consistent with the multifragmentation phenomenon imply a strong radial inhomogeneity in the systems importantly affecting their phase diagrams. Thus, in order to align to the *meaning* of the phase diagrams corresponding to the infinite fluids [11], an extra constraint has to be introduced for the case of the finite systems: *homogeneity*. To this aim, a method for constructing the  $P(V)|_T$  curves corresponding to homogeneous finite systems based on making surface corrections on the bulk virial energy term was designed.

This method makes possible the deduction of the  $P(V)|_T$  curves corresponding to any size of the system,  $A$ , by using the information embedded in the bulk  $P(V)|_T$  curves. The resulting phase diagrams corresponding to homogeneous systems of various sizes show a strong dependence on the size of the system. In this respect, the critical temperature is drastically decreasing when the size of the system is reduced. For example, important deviations from the bulk phase diagram can be noticed even for systems as large as  $A = 10^4$ . This means that the largest equilibrated systems formed in nuclear multifragmentation experiments are not even close to the bulk limit. To this effect one should, of course, couple the inhomogeneity (discussed earlier) and the Coulomb ones. And as shown in Ref. [4] Coulomb is independently bringing a very important contribution towards lowering the system’s critical point.

This work was supported by the Alexander von Humboldt Foundation.

- 
- [1] D. H. E. Gross and E. Votyakov, Eur. Phys. J. **B15**, 115 (2000).
  - [2] P. Borrmann, O. Mulken and J. Harting, Phys. Rev. Lett. **84**, 3511 (2000).
  - [3] Ph. Chomaz, F. Gulminelli and V. Duflot, Phys. Rev. E **64**, 046114 (2001).
  - [4] Al. H. Raduta and Ad. R. Raduta, Phys. Rev. Lett. **87**, 202701 (2001).
  - [5] P. J. Siemens, Nature (London) **305**, 410 (1983); G. Bertsch and P. J. Siemens, Phys. Lett. B **126**, 9 (1983).
  - [6] S. J. Lee and A. Z. Mekjian, Phys. Rev. C **63**, 044605 (2001).
  - [7] H. R. Jaqaman, A. Z. Mekjian and L. Zamick, Phys. Rev. C **29**, 2067 (1984).
  - [8] L. Satpathy, M. Mishra and R. Nayak, Phys. Rev. C, **39**, 162 (1989).
  - [9] Al. H. Raduta and Ad. R. Raduta, Nucl. Phys. **A703**, 876 (2002).
  - [10] J. P. Hansen and L. Verlet, Phys. Rev. **184**, 151 (1969).
  - [11] E. A. Guggenheim, J. Chem. Phys. **13**, 253 (1945).
  - [12] Contributions from the neglected tail to the system’s potential energy and virial energy term [see eq. (4)] are taken respectively as:  
 $\Delta v = \frac{1}{2}\rho A \int_{r_c}^{\infty} dr v(r) = 8\pi\rho A\epsilon[\sigma^{12}/(9r_c^9) - \sigma^6/(3r_c^3)];$   
 $\Delta \mathcal{V} = \frac{1}{2}\rho A \int_{r_c}^{\infty} dr (r \partial v(r)/\partial r) = 8\pi\rho A\epsilon[4\sigma^{12}/(9r_c^9) - 2\sigma^6/(3r_c^3)].$